

Grid Voltage Synchronization of Distributed Generation System under Grid Fault Condition

Mahesh R.Chavhan¹, Prof.Radharaman Shaha²

M.Tech Student, AGPCE, Nagpur, Maharashtra, India¹

HOD, Department of Electrical Engineering, AGPCE, Nagpur, Maharashtra, India²

ABSTRACT: The actual grid code requirements for the grid connection of distributed generation systems, mainly wind and photovoltaic (PV) systems are becoming very demanding. The transmission system operators (TSOs) are especially concerned about the low-voltage-ride-through requirements. Solutions based on the installation of STATCOMs and dynamic voltage regulators (DVRs), as well as on advanced control functionalities for the existing power converters of distributed generation plants, have contributed to enhance their response under faulty and distorted scenarios and, hence, to fulfil these requirements. In order to achieve satisfactory results with such systems, it is necessary to count on accurate and fast grid voltage synchronization algorithms, which are able to work under unbalanced and distributed system conditions. Analysing the synchronization capability of three advanced synchronization systems: the decoupled double synchronous reference synchronous reference frame phase-locked loop (PLL), the dual second order generalized integrator PLL, and the three-phase enhanced PLL, designed to work under such conditions, Although other systems based on frequency-locked loops have also been developed.

KEYWORDS:Electrical variable measurement, electrical engineering frequency estimation, frequency locked loop harmonic analysis, monitoring synchronization.

I. INTRODUCTION

In recent years, there has been an increasing curiosity in electrical power generation from renewable energy sources, such as photovoltaic (PV) or wind power systems. The advent-age of power generation from these sources are widely accept-ed [1]. They are essentially unlimited and environmentally friendly. Among the other renewable-energy sources possible to obtain electricity, solar energy has been one of the most active research areas in the past decennary, both for grid cone-cted and stand-alone applications. The rapid change rate of growth in the worldwide increasing PV capacity is mainly due to increase in grid-connected inverter topologies. AC output voltage is created by switching the full bridge in an appropriate sequence. The inverter topologies can be divided into two types that are the single and multi-stage inverter. The multi-level inverters are applied in high voltage PV power plant mainly due to the high voltage capability, low switching frequency, and low power losses the multilevel topologies include the diode clamped, flying capacitor, and cascaded H-bridge converters. The objective of this paper is to present the modelling and analysis of a novel seven-level inverter for PV and wind power plant application [2]-[3]. STATCOMs and dynamic voltage regulators (DVRs), have played a decisive role in enhancing the fault ride through (FRT) capability of distributed generation systems, as demonstrated in. Likewise, advanced control functionalities for the power converters have also been proposed. In any case, a fast detection of the fault contributes to improving the effects of these solutions; therefore, the synchronization algorithms are crucial. This trend has been followed by the rest of the TSOs; moreover, it is believed that this operation requirement will be extended, and specific demands for balanced and unbalanced sags will arise in the following versions of the grid codes worldwide.

International Journal of Innovative Research in Science, Engineering and Technology

(A High Impact Factor, Monthly, Peer Reviewed Journal)

Visit: www.ijirset.com

Vol. 7, Special Issue 3, March 2018

Unauthorized use of the data set back to the user. Steganography hides the secret message within the host data set and is presence imperceptible and is to be reliably communicated to a receiver. The host data set is purposely corrupted, but in a covert way, designed to be invisible to an information analysis.

II. RELATED WORK

In order to evaluate the response of the grid synchronization topologies, a common performance requirement for all the structures is to be established in this section, considering the needs that can be derived from the LVRT requirements. Despite the fact that the detection of the fault can be carried out with simpler algorithms, as shown, the importance of advanced grid synchronization systems lies in the necessity of having accurate information about the magnitude and phase of the grid voltage during the fault, in order to inject the reactive power required by the TSO.

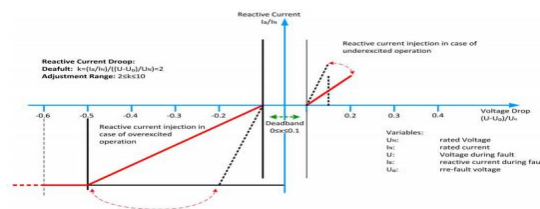


Fig.1 E-on voltage support requirement event of grid fault

A similar condition is given in the Spanish grid code, where the wind power plants are required to stop drawing inductive reactive power within 100 Ms of a voltage drop and be able to inject full reactive power after 150 ms, as shown in Fig.1

A. DDSRF PLL

The DDSRF PLL, published, was developed for improving the conventional SRF PLL. This synchronization system exploits two synchronous reference frames rotating at the fundamental utility frequency, one counterclockwise and another one clockwise, in order to achieve an accurate detection of the positive- and negative-sequence components of the grid voltage vector when it is affected by unbalanced grid faults. When the three-phase grid voltage is unbalanced, the fundamental positive-sequence voltage vector appears as a dc voltage on the dq+ 1 axes of the positive-sequence SRF and as ac voltages at twice the fundamental utility frequency on the dq- 1 axes of the negative-sequence SRF. Finally, the PI controller of the DDSRF PLL works on the decoupled q-axis signal of the positive-sequence SRF (v^*_{q+1}) and performs the same function as in an SRF PLL, aligning the positive-sequence voltage with the d-axis.

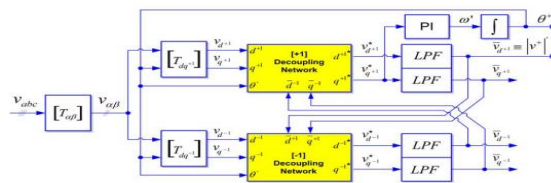


Fig.2 DDSRF-PLL block diagram

B. DSOGI PLL: The operating principle of the DSOGI PLL for estimating the positive- and negative-sequence components of the grid voltage vectors is based on using the instantaneous symmetrical component (ISC) method on the $\alpha\beta$ stationary reference frame as explained. The diagram of the DSOGI PLL is shown in Fig. 3. As it can be noticed, the ISC method is implemented by the positive-sequence calculation block. A conventional SRF PLL is applied on the estimated positive-sequence voltage vector, $v_{\alpha+} \beta+$, to make this synchronization system frequency adaptive. In

International Journal of Innovative Research in Science, Engineering and Technology

(A High Impact Factor, Monthly, Peer Reviewed Journal)

Visit: www.ijirset.com

Vol. 7, Special Issue 3, March 2018

particular, the $v_{\alpha\beta+}$ voltage vector is translated to the rotating SRF, and the signal on the q-axis, v_{+q} , is applied at the input of the loop controller.

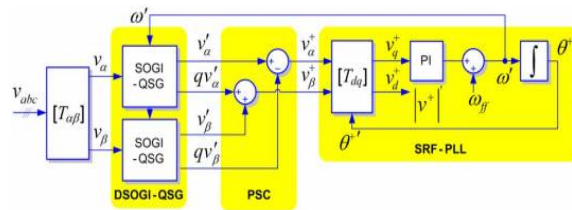


FIG.3 DSOGI-PLL BLOCK DIAGRAM

C. PHEPLL

The enhanced phase-locked loop (EPLL) is a synchronization system that has proven to provide good results in single-phase synchronization systems. An EPLL is essentially an adaptive bandpass filter, which is able to adjust the cut-off frequency as a function of the input signal. Its structure was later adapted for the three-phase case, in order to detect the positive-sequence vector of three-phase signals, obtaining the 3phEPLL that is represented in Fig. 4. In this case, each phase voltage is processed independently by an EPLL.

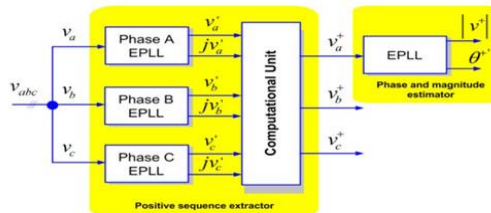


FIG. 3 PHEPLL BLOCK DIAGRAM

III. DISCRETE IMPLEMENTATION:

The performance of the different structures under test is really dependent on their final digital implementation, particularly on the discretization approach made to their continuous equations. This implementation is critical and should be studied in detail as a straightforward implementation can give rise to additional delays in the loop that hinder the good performance of the PLL. Some methods, such as the forward Euler, the backward Euler, and the Tustin (trapezoidal) numerical integration, offer a good performance when used for discretizing other synchronization systems, as shown

A. DDSRF-PLL Discretization

The discrete model of this PLL can be easily obtained since the continuous representation of several parts does not change in the discrete domain.

1) **Positive- and Negative-Sequence Decoupling Networks:** The decoupling network constitutes one of the most important contributions of this synchronization method. The discrete equations of these blocks are shown in (1), being almost the same as in the continuous domain. It is just necessary to consider one sample delay of θ , $v^* d-1$, $v^* q-1$, $v^* d+1$, and $v^* q+1$ in order to avoid algebraic loops.

2) **Phase and Magnitude Estimator Discretization:** In the DDSRF PLL, the decoupling network appears embedded in the classical SRF-PLL loop. However, this does not affect the discretization of the phase and magnitude estimator since $v^* d+1$ and $v^* q+1$ act as the input of this block.

International Journal of Innovative Research in Science, Engineering and Technology

(A High Impact Factor, Monthly, Peer Reviewed Journal)

Visit: www.ijirset.com

Vol. 7, Special Issue 3, March 2018

3) LPF Block Discretization: The amplitudes of the d positive- and negative-sequence components are the outputs of the decoupling networks. However, four infinite impulse responses (IIR) LPFs extract the ripple from each sequence estimation in order to reinforce the performance of the PLL in case of harmonic pollution.

B. DSOGI-PLL Discretization

1) DSOGI-QSG Block Discretization:

As was previously mentioned in Section II, the DSOGI-based quadrature signal generator (QSG) of Fig. 3 consists of two independent and decoupled second-order generalized integrators (SOGIs). Therefore, each SOGI-based quadrature signal generator can be discretised individually, thus facilitating its mathematical description. In Fig. 6, the block diagram of the implemented SOGI is shown.

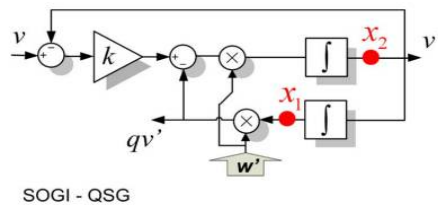


Fig1 Quadrature signal generator based on a second order generalized integrator (SOGI QSG)

2) SRF PLL Discretization:

The frequency and phase detection is obtained by means of the SRF PLL shown in Fig. 8. The discretization of the controller and the integrator is performed using the backward numerical approximation. The frequency and phase can then be represented in the z-domain, as shown in (8), where $v_d + q$ constitutes the error to be minimized.

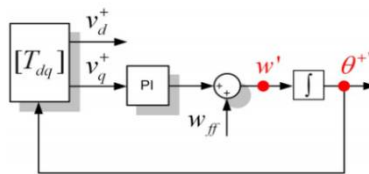


Fig.2 State variables of the SRF-PLL block

C. 3phEPLL Discretization

This three-phase grid synchronization system exploits the EPLL as a quadrature signal generator. An independent EPLL is used for processing each one of the three-phase voltages. The same EPLL structure is applied again to detect the magnitude and phase of the positive-sequence voltage component

1) **QSG Block—EPLL Discretization:** The block diagram of the EPLL implemented in this paper

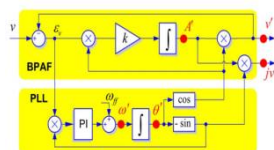


Fig.1 Quadrature signal generator based on an EPLL

International Journal of Innovative Research in Science, Engineering and Technology

(A High Impact Factor, Monthly, Peer Reviewed Journal)

Visit: www.ijirset.com

Vol. 7, Special Issue 3, March 2018

According to this diagram, the state space representation of the EPLL in the continuous domain can be written as shown in

$$\begin{aligned} \dot{A}'(t) &= k \cdot e(t) \cdot \cos \theta'(t) \\ \dot{\omega}'(t) &= -k \cdot e(t) \cdot \sin \theta'(t) \\ \theta(t) &= \omega'(t) + \frac{k_p}{k_i} \cdot \dot{\omega}'(t) \end{aligned}$$

However, for the phase and magnitude detection block, the outputs are the positive sequence magnitude and phase, which correspond directly with the states θ and A , respectively. In the following section, the responses of the DDSRF PLL, DSOGI PLL, and 3PhEPLL under these transient conditions will be compared.

TABLE II
HARMONIC COMPOSITION FOR THE TEST

Order of the harmonic	THD (%)
2 nd	2%
4 th	1%
5 th	5%
7 th	4%
11 th	3%
13 th	3%

Values of individual harmonic voltages at the supply terminals for orders up to 25, given in percent of the nominal supply voltage in RMS

Fig. 6 Hybrid model of solar and wind power system

The hybrid solar–wind system design is mainly dependent on the efficiency of individual components. In order to predict the system’s efficiency, individual components should be modelled first and then their combination can be calculated to meet the demanding reliability

IV. CONCLUSION

Behaviour of three advanced grid synchronization systems. Their structures have been presented, and their discrete algorithms have been studied. The DDSRF PLL and the DSOGI PLL allow estimating the ISCs of a three-phase system working in the $\alpha\beta$ reference frame, while the 3phEPLL uses the “abc” reference frame, thus working with three variables. As has been shown, simplifies the simplifies structure of the DSOGI PLL and the DDSRF PLL, which allows reducing the computational burden, as compared to the 3phEPLL, without affecting its performance. The synchronization capability of the three PLLs under test has been shown to be fast and accurate under faulty scenarios, allowing the detection of the positive sequence of the voltage in 20–25 ms in all cases; however, the simpler structure of the DDSRF and the DSOGI affords an easier tuning of their control parameters and, therefore, a more accurate control of their transient response. The immunity of the analyzed PLLs in the possibility of a polluted network is better when using the 3phEPLL and the DDSRF, due to their greater bandpass and low-pass filtering capabilities. Although the DSOGI also gives rise to reasonably good results, due to its inherent band pass filtering structure, its response is more affected by harmonics. Although all three are appropriate for synchronizing with the network voltage in distributed power generation applications, mainly PV and wind power, the lower computational cost of the DDSRF PLL and the DSOGI PLL, together with their robust estimation of the voltage parameters, offers a better tradeoff between the presented systems, making them particularly suitable for wind power application

A) After doing the literature survey it has been concluded that,

- 1) The behaviour of three advanced grid synchronization systems.

International Journal of Innovative Research in Science, Engineering and Technology

(A High Impact Factor, Monthly, Peer Reviewed Journal)

Visit: www.ijirset.com

Vol. 7, Special Issue 3, March 2018

2) The synchronization capability of the three PLLs under test has been shown to be fast and accurate under faulty scenarios

B) After modelling grid voltage synchronization for distributed generated system under grid fault condition

1) The immunity of the analysed PLLs in the possibility of a polluted network is better when using the 3phEPLL and the DDSRF.

2) Although all three have been shown to be appropriate for synchronizing with the network voltage in distributed power generation applications

REFERENCES

- [1] Zervos and C. Kjaer, Pure Power: Wind Energy Scenarios for 2030. Brussels, Belgium: European Wind Energy Association (EWEA), Apr. 2008
- [2] e-on, "Grid code—High and extra high voltage," Bayreuth, Germany. Apr. 2006
- [3] PO-12.3 Requisitos de Respuesta Frente a Huecos de Tension de las Instalaciones Eolicas, Comisión Nacional de Energía, Madrid, Spain, Oct. 2006
- [4] IEEE Standard for Interconnecting Distributed Resources With Electric Power Systems, IEEE Std. 1547-2003, 2003.
- [5] The Grid Code: Revision 31, National Grid Electricity Transmission, Warwick, U.K., Oct. 2008, no. 3. [Online]. Available: <http://www2.nationalgrid.com/uk/industryinformation/electricity-codes/grid-code/the-grid-code/>
- [6] M. Tsili and S. Papathanassiou, "A review of grid code technical requirements for wind farms," IET Renew. Power Gen., vol. 3, no. 3, pp. 308–332, Sep. 2009.
- [7] F. Iov, A. Hansen, P. Sorensen, and N. Cutululis, "Mapping of Grid Faults and Grid Codes," Risø Nat. Lab., Roskilde, Denmark, Tech. Rep. RisoeR-1617, 2007.
- [8] A. Luna, P. Rodriguez, R. Teodorescu, and F. Blaabjerg, "Low voltage ride through strategies for SCIG wind turbines in distributed power generation systems," in Proc. IEEE PESC, Jun. 15–19, 2008, no. 1, pp. 2333–2339.
- [9] D. Xiang, L. Ran, P. J. Tavner, and S. Yang, "Control of a doubly fed induction generator in a wind turbine during grid fault ride-through," IEEE Trans. Energy Convers., vol. 21, no. 3, pp. 652–662, Sep. 2006.
- [10] J. Morren and S. W. H. de Haan, "Ridethrough of wind turbines with doubly-fed induction generator during a voltage dip," IEEE Trans. Energy Convers., vol. 20, no. 2, pp. 435–441, Jun. 2005